GEOPHYSICAL RESEARCH LETTERS, VOL. 36, L15828, doi:10.1029/2009GL039053, 2009

Impact of sea-surface dust radiative forcing on the oceanic primary production: A 1D modeling approach applied to the West African coastal waters

Marc Mallet,[1,2] Malik Chami,[3] Bernard Gentili,[3] Richard Sempéré,[4] and P. Dubuisson[5]

Received 5 May 2009; revised 24 June 2009; accepted 8 July 2009; published 15 August 2009.

[1] The impact of the dust sea-surface forcing (DSSF) on the oceanic Primary Production (PP) is investigated here by using 1D modelling approach coupling an atmospheric radiative transfer model and a simple PP model. Simulations reveal that dust are able to induce a significant decrease of PP due to the attenuation of light by about 15–25% for dust optical depth (DOD) larger than 0.6–0.7 (at 550 nm). For DOD lower than ~0.2–0.3, the influence of dust on PP is weak (~5%). In addition to DOD, the important role played by dust single scattering albedo (DSSA) is also shown. Realistic applications over the Senegal coast are studied using SeaWiFS and AERONET observations. The analysis showed that PP could be reduced by about 15–20% during the spring period. This study highlights that dust/light interactions need to be parameterized in coupled ocean-atmosphere models used to estimate PP at regional scales.
Citation: Marc, M., M. Chami, B. Gentili, R. Sempéré, and P. Dubuisson (2009), Impact of sea-surface dust radiative forcing on the oceanic primary production: A 1D modeling approach applied to the West African coastal waters, *Geophys. Res. Lett.*, *36*, L15828, doi:10.1029/2009GL039053.

1. Introduction

[2] Although uncertainties still remain, it is recognized that mineral dust are able to influence the biological productivity of the ocean [*Bonnet and Guieu*, 2004; *Cropp et al.*, 2005] through the addition of iron which stimulates photosynthesis by phytoplankton. In parallel to the iron hypothesis, dust aerosols that remain in the atmosphere and are not deposited over oceans are able to significantly reduce the solar energy available at the sea-surface through scattering and absorption processes of incoming solar radiation [*Tanré et al.*, 2003; *Otto et al.*, 2009].

[3] As the growth of phytoplankton biomass depends, in addition to the sources of nutrients, on the availability of light, we explore in this study how the decrease of the Photosynthetically Available Radiation just above the sea-surface (PAR0+) induced by the occurrence of dust in the atmosphere alters the net Primary Production (PP). While the effect of aerosol surface radiative forcing on terrestrial plant productivity [*Mercado et al.*, 2009] has been already investigated, showing a complex balance between the reduction in total PAR (which tends to reduce photosynthesis) and the increase in the diffuse fraction of the PAR (which tends to increase), this study represents, to our knowledge, the first attempt in looking at the potential impact of dust on biological productivity due to dust-radiation processes.

[4] The methodology used in this work (section 2) is based upon a 1D modelling approach which combines a radiative transfer model (RTM) [*Dubuisson et al.*, 2004] together with a PP rate model [*Antoine et al.*, 1996]. Sensitivity analyses were carried out using various and realistic DOD and DSSA, which are two critical optical properties driving DSSF. The 1D simulations are then used together with SeaWiFS and AERONET observations (here aerosol optical depth and angström exponent) over the year 2003 to discuss implications for changes in PP over the West African coast (section 3), which is one of the most intense zones around the world in terms of biological productivity and dust loading.

2. Methodology

2.1. Atmospheric Radiative Transfer Model and Dust Optical Properties

2.1.1. Atmospheric GAME Model

[5] The 1D clear-sky DSSF has been estimated from the multi-spectral atmospheric GAME radiative transfer model [*Dubuisson et al.*, 2004]. GAME accounts for the scattering and absorption processes by particles and gases. The correlated k-distribution method is used for modeling nongray gaseous absorption [*Lacis and Oinas*, 1991]. In this approach, gaseous absorption is accurately approximated using a line-by-line code [*Dubuisson et al.*, 2004], in which the spectroscopic parameters for absorption lines are specified from the HITRAN database [*Rothman et al.*, 2005]. In the line-by-line code, gaseous absorption is calculated at high spectral resolution (about 0.01 cm^{-1} in the shortwave) and for all gaseous species, accounting for the shape and the intensity of each absorption line as a function of pressure and temperature profiles.

[6] Multiple scattering effects are treated using the discrete ordinates method [*Stamnes et al.*, 1988]. This method allows accurate treatment of scattering and absorption by aerosols, clouds, and molecules. GAME has a nominal spectral resolution of 100 cm^{-1} (about 5 nm in the 400–700 nm spectral range). In this study, seven spectral bands (330, 440, 550, 670, 870, 1020 and 1500 nm) have been defined by integrating the spectral fluxes of GAME. Downward net radiative fluxes are calculated over the PAR (0+)

[1] Laboratoire d'Aérologie, Université de Toulouse, Toulouse, France.
[2] Laboratoire d'Aérologie, CNRS, Toulouse, France.
[3] LOV, UMR 7093, UPMC, CNRS, Villefranche sur mer, France.
[4] LMGEM-COM, UMR 6117, Université de la Méditerranée, CNRS, Marseille, France.
[5] LOA, UMR 8518, Université des Sciences et Technologies de Lille I, CNRS, Villeneuve d'Ascq, France.

0094-8276/09/2009GL039053$05.00

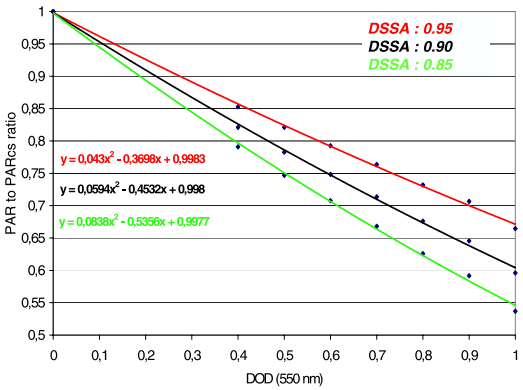

Figure 1. PAR to PARcs ratio simulated versus DOD for three different DSSA (0.85, 0.90 and 0.95). Radiative transfer simulations have been conducted for a zenith angle of 30°.

spectrum (400–700 nm), which corresponds to the range of visible light, for the zenith angle of 30°. Based on these calculated fluxes, DSSF was computed (in W m^{-2}) for different aerosol optical properties.

2.1.2. Aerosol Optical Properties (DOD & DSSA) and Surface Reflectance Used in GAME

[7] The sensitivity analysis was performed using DOD values ranging from 0.4 to 1.0 (at 550 nm), which are typically observed during dust storms. Note that the wavelength 550 nm is selected because it is a central wavelength of the visible spectrum and it is also the wavelength light which is the least absorbed by phytoplankton. The value used for the dust Angström exponent, which is informative of the wavelength spectral dependence of DOD, is 0.3 according to *Dubovik et al.* [2002]. Values of DSSA show significant variability [*Osborne et al.*, 2008; *McConnell et al.*, 2008; *Slingo et al.*, 2006]. Recent in situ measurements report high values of Saharan DSSA (0.95–0.99 at 500 nm) for the accumulation mode [*Osborne et al.*, 2008; *McConnell et al.*, 2008], which contrast with lower values (0.75–0.95 at 500 nm) for bulk dust aerosols [*Slingo et al.*, 2006]. Based on these studies, the simulations were carried out using DSSA values ranging from 0.85 and 0.95 (at 550 nm). DSSA spectral wavelengths dependence over the entire visible spectrum has been taken into account following *Dubovik et al.* [2002].

[8] To compute downward and upward fluxes, the spectral sea-surface reflectance R(0+) was taken into account in the GAME radiative transfer model using the model developed by *Morel* [1988] for three Chlorophyll *a* (Chl) concentrations (0.03, 3 and 10 mg m^{-3}). Note that, for each simulated case, the influence of R(0+) on DSSF was negligible.

2.2. Computation of Primary Production

[9] The model of *Morel* [1991] as adapted by *Antoine and Morel* [1996] for application to satellite data, was used to calculate the oceanic primary production. Briefly, this method allows the computation of primary production within the productive upper layer using the surface chlorophyll concentration measured by an ocean color sensor. It is based on the following general equation [*Morel and Berthon*, 1989]:

$$PP = (1/39)PAR(0+)Chl_{tot}\,\psi^{*} \quad (1)$$

where *PP* is the net carbon fixation within the productive layer (in gC m^{-2}) over a given time interval, PAR(0+) is the photosynthetically available radiant energy at the sea level summed over the spectral range (400–700 nm) per unit of surface (J m^{-2}) over the same time interval, Chl_{tot} is the column integrated chlorophyll content (g Chl m^{-2}). Practically, the computation uses look up tables providing ψ^{*} with date, latitude, surface chlorophyll concentration (Chl) and the sea surface temperature (SST) as input parameters.

[10] The chlorophyll content of the water column is computed from the surface chlorophyll concentration value for two different situations: uniform or stratified biomass vertical profile. The choice of a stratified profile is made when the mixed layer depth is lower than that of the euphotic depth. Details of the methodology are provided by *Antoine et al.* [1995]. Here, the simulations were conducted for parameters representative of the various environmental conditions that can be found in the global ocean. The values of the surface Chl concentrations were 0.03, 0.1, 1 and 10 mg m^{-3}. The uniform and stratified vertical profiles of Chl were used. The sea surface temperature (SST) was varied from 5°C to 30°C by step of 5°C.

3. Results

3.1. Impact of Sea Surface Dust Forcing on Oceanic Primary Production

[11] Figure 1 shows the PAR to $PAR_{clear\text{-}sky}$ ratio as a function of DOD and DSSA, showing clearly the important effect of dust on the surface available light. In parallel, the Figure 2 displays the PP to $PP_{clear\text{-}sky}$ ratio (PP/PP_{cs}) as a function of DOD and DSSA for two values of chlorophyll *a* concentration, namely 1 mg m^{-3} and 10 mg m^{-3}, and two values of SST, namely 10°C and 20°C (the simulations performed for lower Chl concentrations (not shown) indicate relatively similar effects). The results presented here correspond to the stratified vertical profiles. It should be noted that the impact of the vertical profiles on PP/PP_{CS} is low (not shown).

[12] Weak effects of dust on PP are observed when DOD is lower than 0.2–0.3 (~5%, extrapolated from DOD of 0.4 towards lower DOD). The influence of dust increases with the turbidity by ~10% when DOD ranges from 0.4–0.6 and by ~15%–20% when DOD is in the range 0.7–0.9. In all cases, the results underline the importance of the role played by DSSA on PP/PP_{cs}. As an example, when the DOD value is 0.5 (SST of 20°C and Chl of 10 mg m^{-3}) which is a case commonly observed during spring period, PP varies from 3.71 gC m^{-2} day^{-1} to 3.57 gC m^{-2} day^{-1}, for DSSA values of 0.95 and 0.85, respectively. The sensitivity to DSSA clearly increases with DOD and thus, revealing the importance of the dust source mineralogy (iron oxide concentration), which drives DSSA. The effect of DSSF on the PP to PP_{cs} ratio (SST of 20°C and Chl of 10 mg m^{-3}) can be

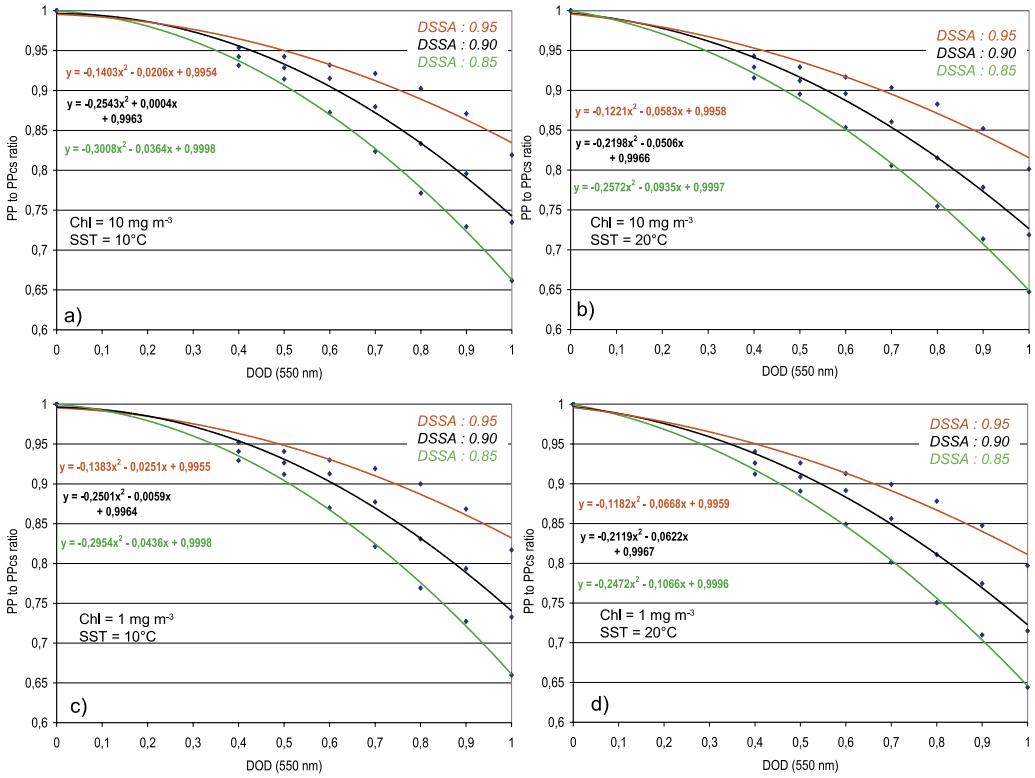

Figure 2. PP to $PP_{clear\text{-}sky}$ (PP_{CS}) ratio simulated versus DOD for two different chlorophyll concentrations, (c and d) 1 and (a and b) 10 mg m^{-3}; two sea surface temperatures, SST of 10 (Figures 2a and 2c) and 20°C (Figure 2b and 2d); and three different DSSA (0.85, 0.90 and 0.95). Simulations presented here correspond to stratified vertical profiles. Polynomial fits linking PP/PPcs with DOD are included in the figures.

parameterized as a function of DOD, for each DSSA, using polynomial fits (Figure 2):

$$PP/PP_{cs} = -0.2572 * DOD^2 - 0.0935 * DOD + 0.9997; \quad (DSSA\ of\ 0.85) r^2 = 0.998 \quad (2)$$

$$PP/PP_{cs} = -0.2198 * DOD^2 - 0.0506 * DOD + 0.9966; \quad (DSSA\ of\ 0.90) r^2 = 0.993 \quad (3)$$

$$PP/PP_{cs} = -0.1221 * DOD^2 - 0.0583 * DOD + 0.9958; \quad (DSSA\ of\ 0.95) r^2 = 0.975 \quad (4)$$

Based on the calculations, DSSF should significantly reduce PP over given regions of interest characterized by significant phytoplankton productivity together with large dust loadings such as the Arabian Sea, the Red Sea and the West African coast. For these regions, the presence of dust is associated both by moderate (∼0.3–0.4 in the Arabian Sea [*Singh et al.*, 2008]) or large (∼0.6–0.8 in the West African coast) DOD. Over these particular regions, the occurrence of dust induces a decrease of the phytoplankton photosynthesis, which is an opposite effect to that induced by an additional input of micro-nutrients such as iron. The competitive contribution between these two effects has to be investigated in a future work.

[13] With regard to aerosol types, moderate effects of DSSF (∼10%) are expected during the dry season (January–March) over the Arabian Sea and the Bay of Bengal, which are characterized by moderate AOD (∼0.3–0.5 [*Ramanathan et al.*, 2001]) and an important net PP (0.50–2 gC m^{-2} d^{-1} [*Antoine et al.*, 1996]). In addition, similar effects are expected over the Yellow Sea and Sea of Japan (AOD ∼ 0.2–0.6 [*Nakajima et al.*, 2007]), Southern Africa (smoke AOD ∼ 0.4–0.7 [*Myhre et al.*, 2003]) and Central Africa during the July–September period. In what follows, the case of the West African coast is discussed.

3.2. Applications to the West African Coast Area

[14] A realistic application of the previous results is investigated over the West African coast using SeaWiFS Chl and SST satellite observations together with ground-based AERONET measurements (DOD and angstrom exponent) at Dakhla (South Morocco) and Dakar (Senegal). The year 2003 is examined because AERONET level 2 data were available for both sites. We focus our study on the spring and summer periods, which correspond to maxima of dust generation over the Saharan region.

[15] Figure 3 shows Chl concentration obtained during those seasons over the Africa continent in 2003. One can observe the high Chl concentration over most of the West African coast with maxima values up to 30–40 mg m^{-3} in spring. In summer, maxima values of Chl are located over the Mauritania and Morocco coastal zones. It should be highlighted that the geophysical products derived from ocean colour satellite sensors (e.g., Chl and other optical

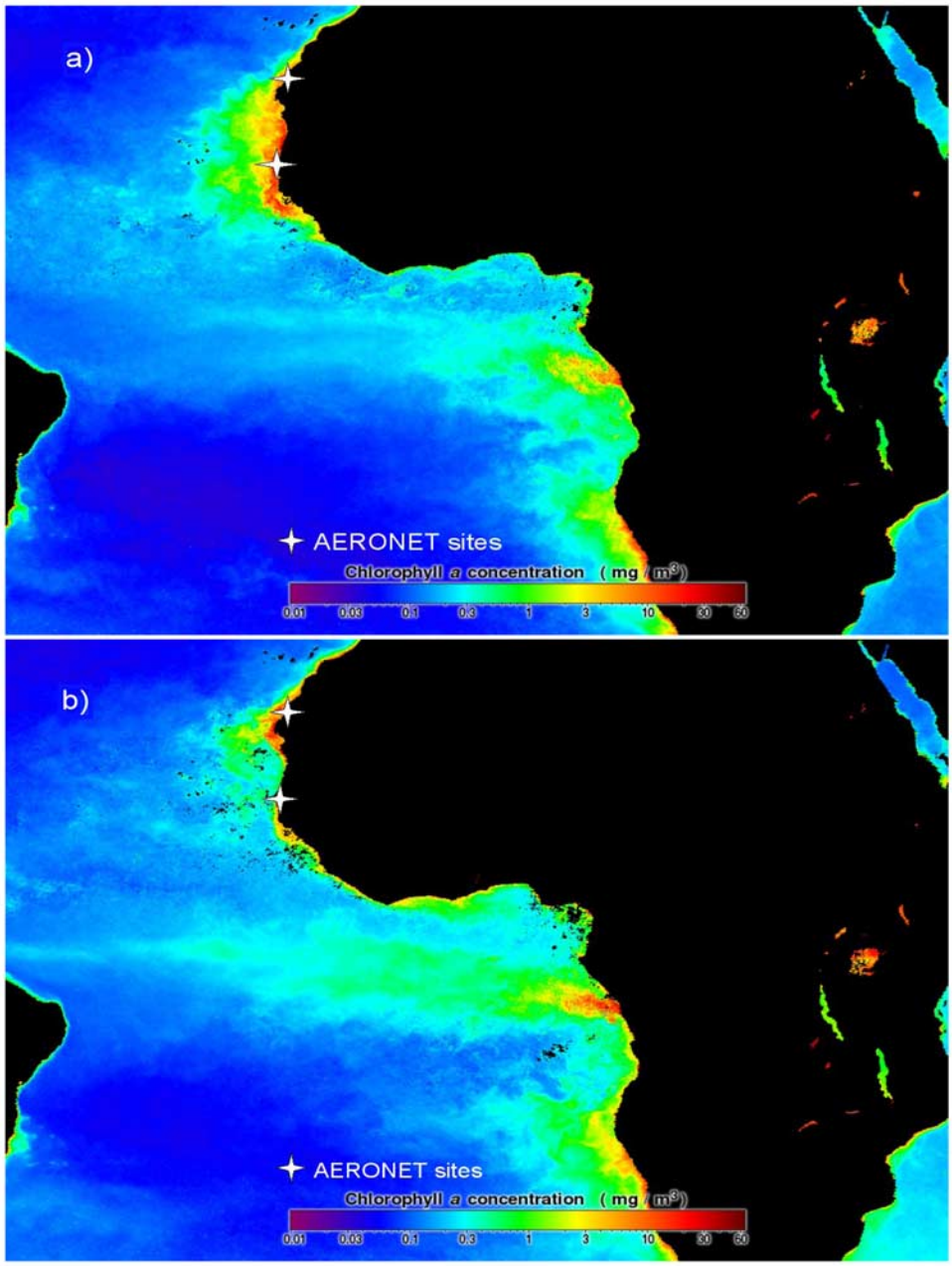

Figure 3. Chlorophyll concentration (in mg m^{-3}) estimated during (a) spring 2003 and (b) summer 2003 by the SeaWifs (http://oceancolor.gsfc.nasa.gov/) sensor over the African continent. The two AERONET sites; Dakar (Senegal) and Dakhla (South Morocco) are indicated by a star.

properties of particles) are probably affected by uncertainties related to the difficulty of making accurate atmospheric corrections of satellite images over optically complex media such as those found in coastal waters and/or in areas characterized by high dust loadings. Despite of the atmospheric correction problem, the satellite images are helpful to provide us with a realistic synoptic view of the spatial variations of the oceanic constituents. Table 1 lists the mean Chl concentration and SST averaged over the Dakhla and Dakar regions for each period.

[16] Table 1 reports the monthly mean and seasonal values of DOD observed at both AERONET sites, revealing significant DOD values between 0.35 and 0.77 at Dakar and

Table 1. Mean SST, Chlorophyll Concentration and Net Primary Production Averaged Over South Morocco and Senegal From SeaWiFS Satellite Observations[a]

	SST (°C)	Chl (mg m^{-3})	PP (gC m^{-2} d^{-1})	DOD (550 nm)	AE (440/870)
			Dakhla		
spring	19.61	4.74	6.26	0.28	0.72
summer	23.11	9.32	6.65	0.47	0.34
			Dakar		
spring	21.10	9.96	6.68	0.71	0.20
summer	27.31	0.83	1.49	0.56	0.32

[a](http://oceancolor.gsfc.nasa.gov/). DOD (level 2) is estimated at Dakhla and Dakar from AERONET. The Angstrom exponent (AE), calculated between the 440 and 870 wavelengths, are also indicated.

between 0.12 and 0.75 at Dakhla. Maxima correspond to the summer time period (July–September) with quite similar values (~0.75 at 550 nm) for each site. In addition, the low values of the Angström exponent (mean of ~0.25 and ~0.5, for Dakar and Dakhla, respectively, Table 1) suggest the occurrence of large particles in the atmosphere and thus, clearly means that extinction of solar radiation is mainly due to dust aerosols in these areas.

[17] Based on such high DOD values and Chl concentrations, the simulations imply that dust could significantly affect the net PP over this region. For example, during the spring period and over the Senegal coast, the net PP could be reduced by about 15% (DSSA of 0.90) or even 20% in cases of more absorbing dust (DSSA of 0.85) due to the high mean value of DOD, namely 0.71. Based on the mean PP value estimated over the Senegal coast (6.7 gC m^{-2} d^{-1}), it is expected from the calculations that dust could decrease PP by about ~1.0 gC m^{-2} d^{-1} in spring. Similar effects could be expected at Dakhla especially in summer, when high Chl concentrations (9.32 mg m^{-3}) are associated with large DOD (0.47).

[18] Note that highly absorbing dust in the blue could also have an impact on PP. Typically, if all the blue light is being attenuated by dust making the sky appearing red, the spectral quality of PAR will be significantly changed and the impact on photosynthesis is likely to be measurable because of the action spectrum of phytoplankton being peaked in the blue. Such an effect should be possibly modelled, especially if a spectral type of model of PP is employed. This is an obvious channel for further investigation. Therefore, the analysis of our results indicate that DSSF could produce a non negligible negative effect (opposite to the one due to the addition of soluble iron either from deposition or upwelling) in the stimulation of the phytoplankton photosynthesis over the West African coast during summer and spring.

[19] Therefore, this study suggests that regional coupled Ocean-Atmosphere models should take into account the possible influence of DSSF on oceanic PP over regions that are characterized by a strong biological productivity and dust loading such as those previously mentioned. Furthermore, it should be highlighted that such developments could be of great interest for treating the potential impact of DSSF on SST, which consists in a decrease of about ~2–3°C during dust storms [*Foltz and McPhaden*, 2008; *Singh et al.*, 2008]. Such a specific effect (which was not addressed here) is directly related to DSSF and may also alter net PP.

4. Conclusion

[20] A 1D modelling approach was conducted to investigate the influence of dust sea surface forcing on the oceanic primary production. The results showed that dust can cause a non negligible decrease in PP, which is attributed to the decrease of the sea-surface illumination. Reduction in PP could reach 15–25% for dust optical depth larger than 0.6, while a weaker effect (~5%) is observed for lower values (DOD < 0.4). Polynomial fits were proposed to parameterize the variations in the primary production with respect to the optical properties of dust aerosols. Simulations also revealed that the impacts of DSSF on PP are expected to be restricted to few geographic areas such as the Red Sea, the Arabian Sea and the West African coastal waters. As an example, it was shown that the net PP could be reduced by about 15–20% (~1.0 gC m^{-2} d^{-1}) over the Senegal region in spring. This study suggests that DSSF can not be ignored in coupled atmosphere-ocean models for calculating accurately PP and thus, to gain an understanding in the carbon cycle and the climate change effects. The parameterization established here between the primary production and the dust optical depth might be used to account for the influence of dust sea surface forcing on the biological productivity.

[21] **Acknowledgments.** We gratefully acknowledge D. Tanré, H. Benchekroun and B. Holben, who are in charge of the Dakar and Daklha AERONET sites.

References

Antoine, D., and A. Morel (1996), Oceanic primary production: I. Adaptation of a spectral light-photosynthesis model in view of application to satellite chlorophyll observations, *Global Biogeochem. Cycles*, *10*, 43–55, doi:10.1029/95GB02831.

Antoine, D., A. Morel, and J. M. André (1995), Algal pigment distribution and primary production in the eastern Mediterranean as derived from coastal zone color scanner observations, *J. Geophys. Res.*, *100*, 16,193–16,209, doi:10.1029/95JC00466.

Antoine, D., J. M. André, and A. Morel (1996), Oceanic primary production: II. Estimation at global scale from satellite (coastal zone color scanner) chlorophyll, *Global Biogeochem. Cycles*, *10*, 57–69, doi:10.1029/95GB02832.

Bonnet, S., and C. Guieu (2004), Dissolution of atmospheric iron in seawater, *Geophys. Res. Lett.*, *31*, L03303, doi:10.1029/2003GL018423.

Cropp, R. A., A. J. Gabric, H. McTanish, R. D. Braddock, and N. Tindale (2005), Coupling between ocean biota and atmospheric aerosols: Dust, dimethylsulphide or artefact?, *Global Biogeochem. Cycles*, *19*, GB4002, doi:10.1029/2004GB002436.

Dubovik, O., B. N. Holben, T. F. Eck, A. Smirnov, Y. J. Kaufman, M. D. King, D. Tanré, and I. Slutsker (2002), Variability of absorption and optical properties of key aerosol types observed in worldwide locations, *J. Atmos. Sci.*, *59*, 590–608, doi:10.1175/1520-0469(2002)059<0590:VOAAOP>2.0.CO;2.

Dubuisson, P., D. Dessailly, M. Vesperini, and R. Frouin (2004), Water vapor retrieval over ocean using near-infrared radiometry, *J. Geophys. Res.*, *109*, D19106, doi:10.1029/2004JD004516.

Foltz, G. R., and M. J. McPhaden (2008), Impact of Saharan dust on tropical North Atlantic SST, *J. Clim.*, *21*, 5048–5060, doi:10.1175/2008JCLI2232.1.

Lacis, A. A., and V. Oinas (1991), A description of the correlated k-distribution method, *J. Geophys. Res.*, *96*, 9027–9064, doi:10.1029/90JD01945.

McConnell, C. L., E. J. Highwood, H. Coe, P. Formenti, B. Anderson, S. Osborne, S. Nava, K. Desboeufs, G. Chen, and M. A. J. Harrison (2008), Seasonal variations of the physical and optical characteristics of Saharan dust: Results from the Dust Outflow and Deposition to the Ocean (DODO) experiment, *J. Geophys. Res.*, *113*, D14S05, doi:10.1029/2007JD009606.

Mercado, L. M., et al. (2009), Impact of changes in diffuse radiation on the global land carbon sink, *Nature*, *458*, 1014–1017, doi:10.1038/nature07949.

Morel, A. (1988), Optical modelling of the upper ocean in relation to its biogenous matter content (case 1 waters), *J. Geophys. Res.*, *93*, 10,749–10,768, doi:10.1029/JC093iC09p10749.

Morel, A. (1991), Light and marine photosynthesis: A spectral model with geochemical and climatological implications, *Prog. Oceanogr.*, *26*, 263–306, doi:10.1016/0079-6611(91)90004-6.

Morel, A., and J. F. Berthon (1989), Surface pigments, algal biomass profiles, and potential production of the euphotic layer: Relationships reinvestigated in view of remote sensing applications, *Limnol. Oceanogr.*, *34*, 1541–1564.

Myhre, G., T. K. Berntsen, J. M. Haywood, J. K. Sundet, B. N. Holben, M. Johnsrud, and F. Stordal (2003), Modeling the solar radiative impact of aerosols from biomass burning during the Southern African Regional Science Initiative (SAFARI-2000) experiment, *J. Geophys. Res.*, *108*(D13), 8501, doi:10.1029/2002JD002313.

Nakajima, T., et al. (2007), Overview of the Atmospheric Brown Cloud East Asian Regional Experiment 2005 and a study of the aerosol direct

radiative forcing in east Asia, *J. Geophys. Res.*, *112*, D24S91, doi:10.1029/2007JD009009.

Osborne, S. R., B. T. Johnson, J. M. Haywood, A. J. Baran, M. A. J. Harrison, and C. L. McConnell (2008), Physical and optical properties of mineral dust aerosol during the Dust and Biomass-burning Experiment, *J. Geophys. Res.*, *113*, D00C03, doi:10.1029/2007JD009551.

Otto, S., et al. (2009), Solar radiative effects of a Saharan dust plume observed during SAMUM assuming spheroidal model particles, *Tellus, Ser. B*, *61*, 270–296, doi:10.1111/j.1600-0889.2008.00389.x.

Ramanathan, V., et al. (2001), Indian Ocean Experiment: An integrated analysis of the climate forcing and effects of the great Indo-Asian haze, *J. Geophys. Res.*, *106*(D22), 28,371–28,398, doi:10.1029/2001JD900133.

Rothman, L. S., et al. (2005), The HITRAN molecular spectroscopic database, *J. Quant. Spectrosc. Radiat. Transf.*, *96*, 139–204, doi:10.1016/j.jqsrt.2004.10.008.

Singh, R. P., A. K. Prasad, V. K. Kayetha, and M. Kafatos (2008), Enhancement of oceanic parameters associated with dust storms using satellite data, *J. Geophys. Res.*, *113*, C11008, doi:10.1029/2008JC004815.

Slingo, A., et al. (2006), Observations of the impact of a major Saharan dust storm on the atmospheric radiation balance, *Geophys. Res. Lett.*, *33*, L24817, doi:10.1029/2006GL027869.

Stamnes, K., S. Tsay, W. Wiscombe, and K. Jayaweera (1988), Numerically stable algorithm for discrete-ordinate-method radiative transfer in multiple scattering and emitting layered media, *Appl. Opt.*, *27*, 2502–2509, doi:10.1364/AO.27.002502.

Tanré, D., et al. (2003), Measurement and modeling of the Saharan dust radiative impact: Overview of the SaHAran Dust Experiment (SHADE), *J. Geophys. Res.*, *108*(D18), 8574, doi:10.1029/2002JD003273.

M. Chami and B. Gentili, LOV, UMR 7093, UPMC, CNRS, BP 8, F-06238 Villefranche sur mer CEDEX, France.

P. Dubuisson, LOA, UMR 8518, Université des Sciences et Technologies de Lille I, CNRS, F-59655 Villeneuve d'Ascq CEDEX, France.

M. Mallet, Laboratoire d'Aérologie, Université de Toulouse, 14 avenue Edouard Belin, F-31400 Toulouse CEDEX, France. (malm@aero.obs-mip.fr)

R. Sempéré, LMGEM-COM, UMR 6117, Université de la Méditerranée, CNRS, F-13288 Marseille CEDEX 9, France.